In situ x-ray diffraction measurements of the c/a ratio in the high-pressure ϵ phase of shock-compressed polycrystalline iron

James A. Hawreliak,* Bassem El-Dasher, and Hector Lorenzana
Lawrence Livermore National Laboratory, Livermore, California 94550, USA

Giles Kimminau, Andrew Higginbotham, Bob Nagler, Sam M. Vinko, William J. Murphy, Thomas Whitcher, and Justin S. Wark
Department of Physics, Clarendon Laboratory, University of Oxford, Parks Road, Oxford OX1 3PU, United Kingdom

Steve Rothman and Nigel Park
AWE Aldermaston, Reading, United Kingdom

(Received 5 January 2010; revised manuscript received 9 December 2010; published 27 April 2011)

The structure of laser-shock-compressed polycrystalline iron was probed using *in situ* x-ray diffraction over a pressure range spanning the α-ϵ phase transition. Measurements were also made of the c/a ratio in the ϵ phase, which, in contrast with previous *in situ* x-ray diffraction experiments performed on single crystals and large-scale molecular dynamics (MD) simulations are close to those found in high-pressure diamond anvil cell experiments. This is consistent with the observation that significant plastic flow occurs within the nanosecond time scale of the experiment. Furthermore, within the sensitivity of the measurement technique, the fcc phase that had been predicted by MD simulations was not observed.

DOI: 10.1103/PhysRevB.83.144114 PACS number(s): 62.50.Ef, 61.05.cp, 61.46.Hk, 61.72.Hh

I. INTRODUCTION

The high-pressure states of iron have long been of interest, in no small part due to iron's geophysical and technological importance. One of the most studied parts of the phase diagram is the α-ϵ (bcc to hcp) transition that occurs around 13 GPa.[1] Indirect evidence for this transition was observed in shock compression experiments,[2,3] with the atomic structure determined later for static high-pressure samples using x-ray diffraction.[4,5] It has recently been found that, at least on nanosecond time scales for high-quality single crystals of iron shocked along the [100] axis, the transformation to the ϵ phase occurs in such a way that the c/a ratio exceeds 1.7,[6,7] which is far higher than those found in diamond anvil cell (DAC) experiments where the majority of reported values cluster around 1.61 (close to the ideal hcp value of 1.63), although variations have been reported as a function of pressure, with upper and lower limits of 1.67 and 1.59, respectively.[8] The large c/a values can be explained by the lack of plasticity observed in the shock-loaded single crystals on the time scale of these experiments leaving the interplanar spacings of the $\{011\}$ planes orthogonal to the loading axis unchanged (which became the c axes of the material in the ϵ phase). These remarkable findings were in excellent agreement with large-scale molecular dynamics (MD) simulations,[9] which simulated the shock process for several tens of picoseconds. Simulations of single crystals of iron shocked along the [110] and [111] directions to above the transition pressure contain a large fraction of fcc as well as hcp, the γ and ϵ phases, respectively.[10] Due to the orientation dependence, a significant fraction of fcc phase has also been predicted to be found in shock-compressed polycrystalline iron,[11] where the values of the c/a ratio are closer to the ideal value at 1.633.[12] It is in this context that we report experimental data where we used *in situ* x-ray diffraction to measure the structure and the c/a ratio of laser-shock-compressed polycrystalline iron. In agreement with the MD simulations, we find c/a ratios of 1.61 ± 0.01 that are now very similar to those found in DAC experiments. However, we find no evidence of an fcc phase.

II. EXPERIMENTAL METHOD

The experiments were performed at the U.K. STFC VULCAN laser facility.[13] The x rays diffracted from the shocked iron foils were recorded by use of a cylindrical polycrystalline pinhole camera (CPPC)[14] shown in Fig. 1. In this geometry, a collimated x-ray source and the shocked sample to be interrogated are placed on the axis of a cylinder, on the inside surface of which is placed a Fuji SR imaging plate. A nanosecond 100-μm-diameter source of quasimonochromatic x rays was produced by using a high-power optical (532-nm) laser to illuminate a 12.5-μm-thick iron foil at an irradiance of $\sim 10^{14}$ W cm^{-2}. This resulted in the generation of iron K-shell radiation from the resonance line of heliumlike Fe at a central wavelength of 1.85 Å. These x rays were collimated by a brass tube coaxial with the cylinder resulting in x-ray illumination of ~ 1 mm^2 on the shocked sample with an angular divergence of $\sim 0.5^\circ$, at an angle of 45° to the cylinder axis.

The material was 25-μm-thick polycrystalline-rolled iron obtained from GoodFellow. An electron backscatter diffraction analysis showed that the foils were textured, with [110] planes having their plane normals lying preferentially along the normal to the target surface. The grain size was typically on the order of $10 \times 10 \times 50$ μm, with the long axis lying along the direction of rolling. The foils were overcoated with 20-μm paralyne N, and then 100 nm of aluminum, with the foils being shocked by laser irradiation of the Al surface. The foils were irradiated by a 6-ns-long trapezoidal laser pulse with rise and fall times of 100 ps. The focal spot on the iron foils was 8 mm^2, and the foils were irradiated at laser intensities between 1×10^{11} and 1.2×10^{12} W cm^{-2} with 1064-nm radiation,

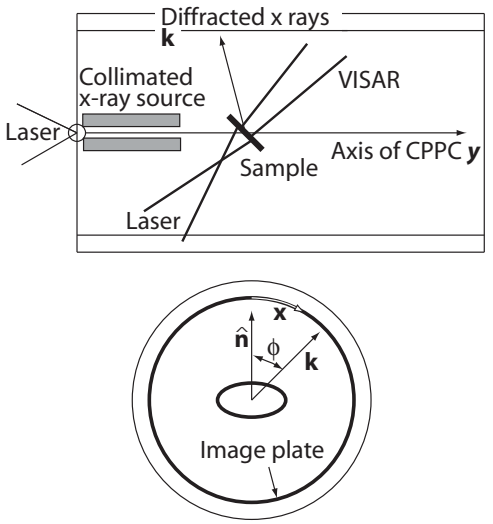

FIG. 1. Schematic of the experimental setup. The sample is oriented such that the plane normal makes an angle $i = 45^\circ$ to the axis of the cylinder and incoming x rays. The drive laser beam is defocused to give a drive spot 2 mm in diameter. The deflection angle 2θ is measured with respect to the axis of the CPPC.

generating shock pressures ranging from 8 to 60 GPa. The shock pressures were deduced from velocity interferometer (VISAR) measurements reflecting from the rear free surface of the foil with a separate laser wavelength of 532 nm, synchronized to the shock-driving laser.[15] The measured free-surface velocity was divided by 2 to get the particle velocity at the rear surface, and then, the pressures were inferred from standard Hugoniot tables for iron.[16] Owing to the finite-temporal resolution of the system, no multiple wave structure was observed in the VISAR signals, and, thus, for those shots where we see both α and ϵ phases in the diffraction, we cannot assign a lower pressure to a distinct wave of compressed α phase, and the pressure quoted is presumed to correspond to peak pressure in the system.

The relative delay between the 1-ns laser pulse used to generate the x rays and the shock-driving beam was set such that the x-ray pulse ended before the shock reached the rear surface of the foil. Because the shock did not totally traverse the foil at the time of the x-ray pulse, a record of diffraction from both unshocked and shocked regions was obtained as the attenuation length of the x rays, $\approx 20\ \mu$m, was of the same order as the thickness of the foil. The diffraction from the unshocked material allows accurate calibration of the instrument on a shot-to-shot basis. An example of the raw image plate data for a foil shocked to above the transition pressure is shown in Fig. 2(a). There is a strong variation in the diffracted intensity as a function of ϕ owing both to the response function of the instrument[14] and to the degree of texture of the foil.

III. RESULTS

In Fig. 2(b), we show line outs of the diffracted x rays (with background subtracted) for an unshocked sample, a 10-GPa loading, and a 15-GPa loading, which are below and above the transition pressure, respectively. It can be seen that, for the

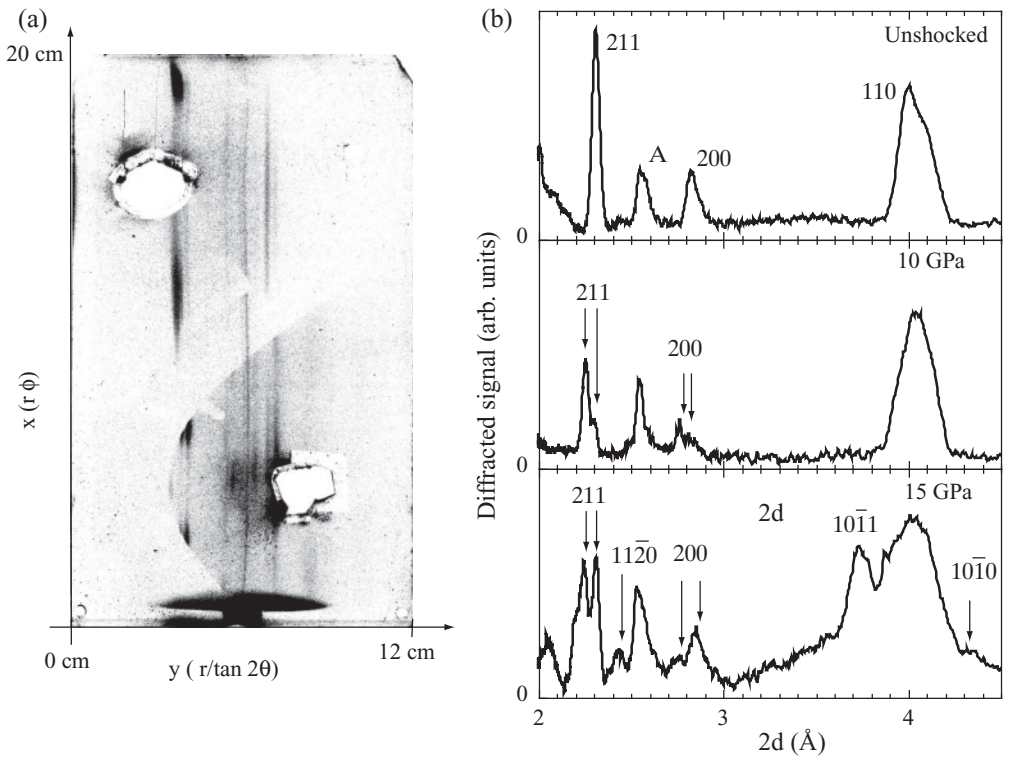

FIG. 2. (a) An example of raw data for a foil shock compressed to 15 GPa (as determined by VISAR) showing diffraction from both hcp and bcc structures. (b) Integrated line outs with the background subtracted for pressures of 0, 10, and 15 GPa. The relevant peaks used in the structural determination are labeled; the feature marked A is diffracted from the collimating tube.

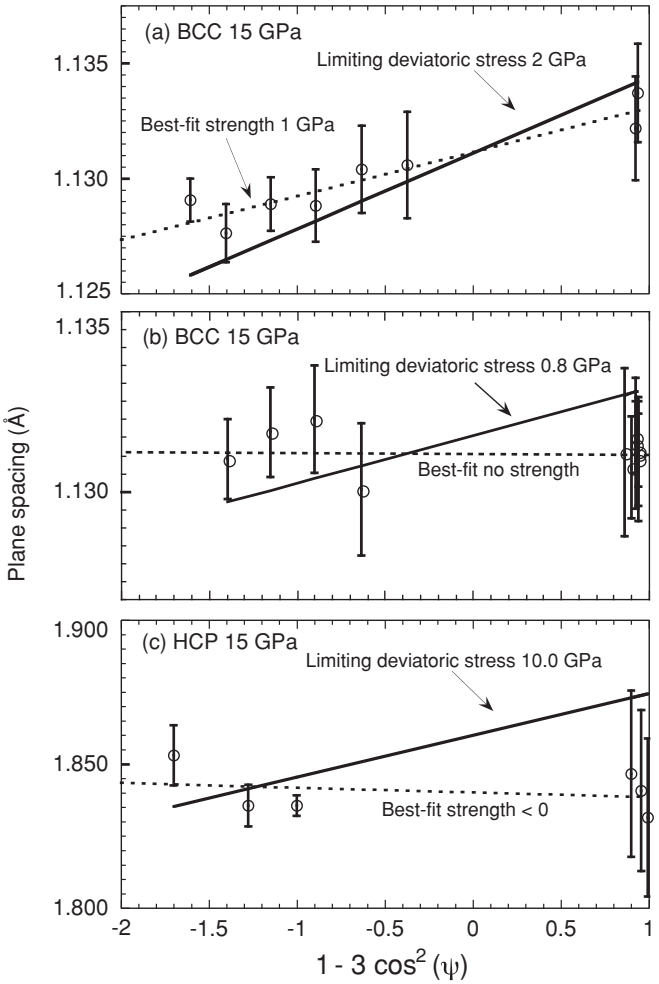

FIG. 3. (a), (b) A plot of lattice compression as a function of angle for (112) bcc at 15 GPa on two different shots, showing behavior consistent with low levels of strength. (c) A plot of hcp $(10\bar{1}1)$ showing a limiting strength of 10 GPa, although a best fit to close to zero strength.

15-GPa pressure, new diffraction features appear, which we have labeled as diffraction from the $(10\bar{1}1)$ and $(11\bar{2}0)$ reflections of the hcp phase (we give reasons for these identifications below). As the target is placed at an angle i (in this case, $\pi/4$) to the incident x rays, a reflection at a given (θ,ϕ) corresponds to diffraction from grains that have plane normals at an angle ψ with respect to the shock propagation direction given by $\cos\,\psi = (\cos\,\theta\,\cos\,\phi\,\sin\,i - \sin\,\theta\,\cos\,i)$.[14] We can fit the data to the standard formula for determining material strength from diffraction 1–3 $\cos^2(\psi)$, assuming isostress across the grain boundaries (Ruess limit), shown in Fig. 3.[17,18] In this form, the lattice plane spacing is given by $d_{(hkl)}(\psi) = d_{(hkl)}\{1 + [1–3\,\cos^2(\psi)]Q(hkl)\}$, where $d_{(hkl)}$ and $d_{(hkl)}(\psi)$ are the plane spacing based on hydrostatic compression at this pressure and the plane spacing at the angle ψ including strength, and $Q(hkl)$ is a plane-specific term that is calculated using the strength, the elastic constants, and the lattice geometry.[17,18] We can fit the data using a standard least-squares fit and estimate the limiting values of strength in the material using pressure-scaled elastic constants.[19,20] The error bars represent one standard deviation from a least-squares fit to the peak location. The value of strength for the bcc phase at 15 GPa is 1 ± 1.5 GPa, which includes the hydrostatic limit, i.e., no strength. In the hcp phase, the error bars are too large to make a reasonable estimate of strength.

Given that the angular position of the $(10\bar{1}1)$ reflection is sensitive to both lengths of the c and a axes, while the position of the $(11\bar{2}0)$ peak depends only on the a axis, we can deduce the c/a ratio. From an analysis of these two peaks, we deduce $c/a = 1.61 \pm 0.01$ for all shots where the ϵ phase was observed and see no variation as a function of pressure. Using an hcp crystallographic structure with a c/a ratio of 1.61 also predicts the feature seen on the shoulder of the (110) static peak, identified as the $(10\bar{1}0)$ plane in Fig. 2(b).

Several factors allow identification of the new lines as being consistent with the hcp phase (rather than fcc, or simply, the compressed bcc lattice). First, the new reflection that we label as $(11\bar{2}0)$ hcp lies to the low angle side of the (112) bcc reflection from the uncompressed lattice. The shock-compressed bcc lattice in this region is seen clearly at the high angle (compression) side. As rarefaction has not occurred (as verified by the timing of shock from VISAR), the reflection cannot correspond to a bcc or a body-centered-tetragonal crystal. Furthermore, it is impossible to reconcile the two lines labeled as hcp with a single fcc density, while an hcp structure with a c/a ratio of 1.61 can produce both lines at a density consistent with the appearance of the new lines. Diffraction from a (220) fcc plane at a density within the error of the VISAR measurements can be consistent with diffraction-labeled $(11\bar{2}0)$ hcp, but this structure does not explain either the $(10\bar{1}1)$ or the $(10\bar{1}0)$, and there is no signal where we would expect to see (110) fcc and (200) fcc diffraction.

In Fig. 4, we plot the densities as a function of pressure (as deduced from the VISAR data) for both material phases with the shock Hugoniot obtained from gas-gun results.[16,21] It can be seen that, for the two data points in the low-pressure regime, below the transition pressure denoted on the plot by hollow squares, where only the compressed bcc lattice is seen in the diffraction, there is good agreement with standard Hugoniot measurements. Similarly, at high pressures, where only the hcp phase is observed in diffraction (consistent with total transformation of the lattice on the time scale of the experiment), agreement is also good, although in this regime, the error bars are larger. Interestingly, within the transition regime between 13 and 30 GPa, there is a tendency for the densities deduced via diffraction to be lower than the bulk Hugoniot data for the compressed bcc phase but greater than it for the hcp phase. Such an observation is consistent with a model where the main shock wave within the material is a mixture of the two phases, with the hcp regions having a higher mean density and the bcc at a lower density so the net average density falls on the Hugoniot. This is similar to the two-phase region observed in static experiments between 13 and 18 GPa.[8] In principle, the fraction of the material that has been transformed to the hcp phase can be deduced from the intensity of the relevant diffraction peaks. However, such an analysis is severely complicated in the current experiments owing both to the low level of signal to noise in the data and by the high degree of texture within the sample.

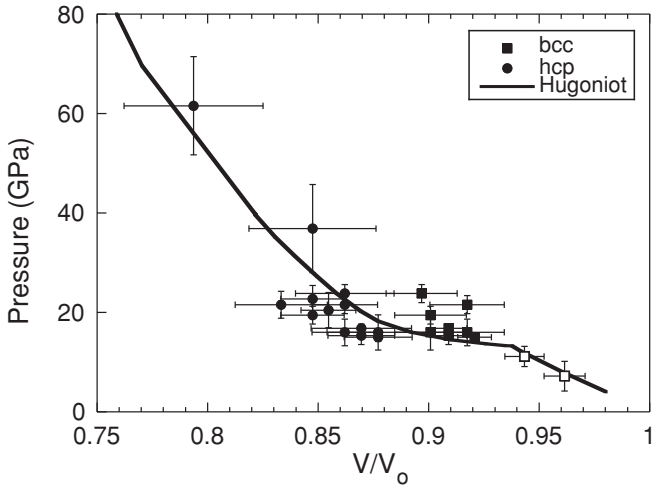

FIG. 4. A P-V plot of the iron-shock Hugoniot. Pressure is interpreted from free-surface velocity measurements made by VISAR, and volume is measured using x-ray diffraction. The bcc structure is marked with squares where the hollow ones denote diffraction when only the bcc phase was observed, while the hcp is marked with circles, and the gas-gun Hugoniot is plotted as a solid line. In the transition region, the plot shows (13–30 GPa) where both bcc and hcp phases are observed in the diffraction at densities that do not lie on the Hugoniot.

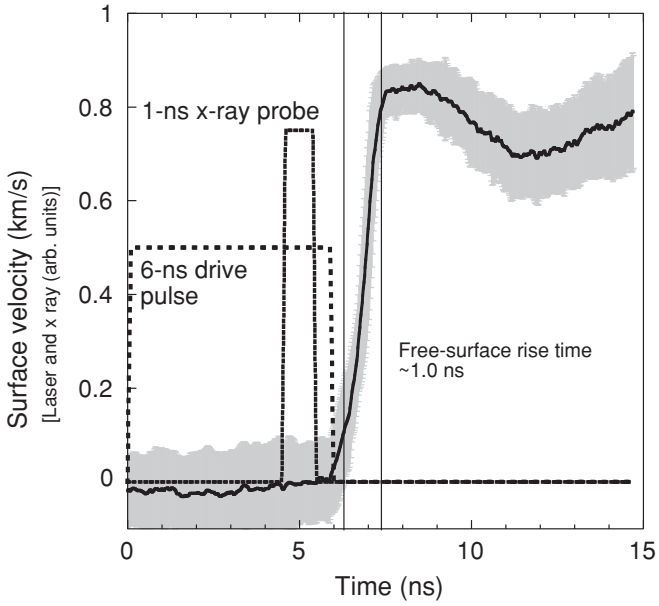

FIG. 5. Free-surface velocity measurements from experiment with diffraction shown in Fig. 2.

IV. DISCUSSION

We have shown, using *in situ* x-ray diffraction, that shock-loaded polycrystalline iron foils undergo the α-ϵ phase transition on a nanosecond time scale. The use of a laser to ablatively shock load a sample has the advantage that it requires very little infrastructure around the target, allowing wide angle diagnostics, such as x-ray diffraction using the CPPC to be used *in situ*. For the experiments performed here, the rolled-iron foils were 25-μm thick, which was required for the sample to be thin enough for the 6.7-keV x-ray backlighter to volumetrically probe the target and is also thin enough to have a supported shock wave with the available laser energies and pulse shapes. At pressures below the phase transition, the Bland number is $L/\delta \approx 1/100$,[22] where L is the sample thickness and δ is the distance required to establish a steady shock ($\approx$3 mm). A Bland number greater than 1 means a steady shock will be generated within the sample. For our experiments, we were not in the steady shock regime. We have a strain rate about an order of magnitude faster than would be observed in a steady front at the back of a thick sample. Figure 5 shows the free-surface velocity data for the diffraction image shown in Fig. 2. In this figure, we have denoted the relative timing of laser pulses associated with the loading of the sample and the x-ray probe. The break out shows a 1.0-ns rise time, including the 260-ps round-trip time associated with the 50-mm-thick etalon, followed by a flat velocity region for $\approx$1.5 ns. Swegle-Grady determined a steady-state strain rate on 6.3-mm samples below the transition of 4×10^6 s^{-1} at 13.2 GPa;[23] using a similar analysis of the wave profile, the strain rate in our experiment is 1×10^8 s^{-1} at 15 GPa with no obvious correlation to pressure. The strain rate at the front of the sample would most likely be higher as the shock-wave profile approaches the steady profile through the sample.[24] In Fig. 6, we plot the time scale associated with the Swegle-Grady relation as

$$t_{\mathrm{SG}} = \frac{1 - (v/v_o)_{\mathrm{Hugoniot}}}{\dot{\epsilon}_{\mathrm{SG}}} \tag{1}$$

where $\dot{\epsilon}_{\mathrm{SG}} = 137\sigma^4$, $(v/v_o)_{\mathrm{Hugoniot}}$ is taken for the Hugoniot, and the rise times are taken from these experiments and are plotted as a function of pressure. It is clear that the points below the transition, denoted as hollow squares, are an order of magnitude faster time scale then Swegle-Grady would predict for a steady wave.

In these experiments, the strain rate driving the pressure wave is larger than that which would exist in the steady shock case. As a result, we would expect the state resulting from the rapid compression to have a higher entropy than a steady shock for the same pressure.[24] This will manifest itself as a lower density at a given pressure than on the steady shock Hugoniot. Although we are not in the steady shock regime, low-pressure experimental data suggest that the deviation in density from the Hugoniot for a given particle speed is smaller than the error bars for the measurements. The two points we measure below the phase transition (denoted with hollow squares) in Fig. 4 compare very well with the standard Hugoniot for iron. This deviation would be largest there as the Bland number would be the lowest for the lowest pressures, so within our experimental uncertainty, the Hugoniot does not depend on the strain rate. With higher-fidelity density measurements, it may be possible to actually resolve the difference in density due to the increase in entropy.

In hydrodynamic models, the deviation of the shock front from an ideal discontinuity to a finite-rise time is associated with an effective material viscosity that can be thought of as being responsible for the observed SG fourth-order

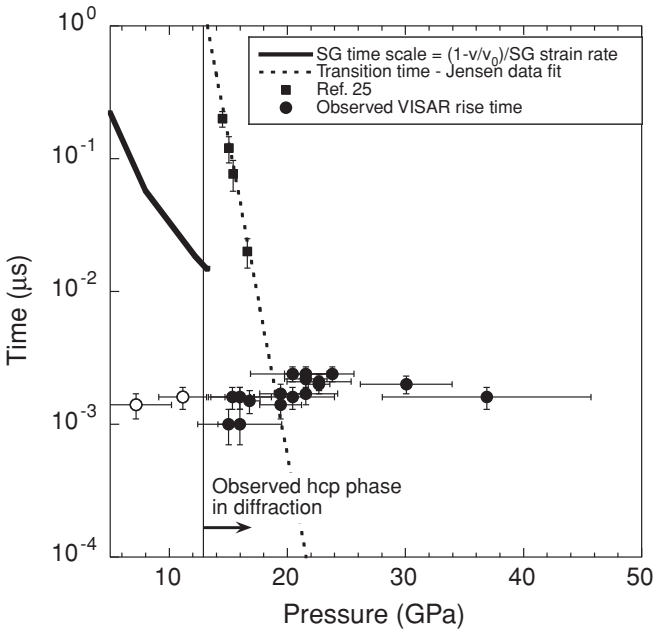

FIG. 6. A time versus pressure plot of the Swegle-Grady relation for iron, the transition time scale from Ref. 25, and the rise time of the free-surface velocity for the laser experiments where the hollow circles denote points where no hcp was observed in the diffraction.

power law.[23] In many shock-wave experiments, this effective viscosity has been interpreted as a material kinetic process, such as the formation and movement of dislocations during plastic relaxation or the rearranging of atoms during a phase transition. The *in situ* x-ray diffraction measurements shown above provide direct measures of atomic structure that show that the time scales associated with these material processes are much faster than those associated with the rise time in a steady shock. Below the phase transition, points denoted by hollow squares in Figs. 4 and 6 show nearly hydrostatic relaxation of the lattice, with no obvious signs of elastic compression in the diffraction. Similarly, above the transition pressure, we see a prompt formation of the hcp phase in a significant fraction to suggest it is a major component of the material. In both cases, the observation in the x-ray diffraction suggests the material time scale of plastic relaxation, and phase transition occurs much faster than previously interpreted from the rise time of steady shocks. In Fig. 6, we plot the transition time scale Jensen *et al.*[25] interpreted from relaxations in the velocity profile at the shock interface. While the majority of data agrees with the transition time-scale model proposed by Jensen *et al.*, we do not observe the same time dependence at the lower pressures; the exact cause of this difference is uncertain because of the different strain rates and target configurations of the two experiments. An ideal future experiment, using x-ray diffraction, would be to look at the material structure and the relaxation velocity at the front surface for pressure just above the transition pressure to correlate atomistic material behavior with bulk material behavior. These measurements stress the importance of *in situ* probing of dynamic experiments to provide a better understanding of material processing.

In conclusion, we have shown that nanosecond x-ray diffraction can be used to study the structure of polycrystalline iron during a shock-induced phase transition. Importantly, our data are not consistent with an fcc structure in the high-pressure phase, as has been predicted by MD for shocked polycrystalline samples. We note, however, that the time scale of the experiments reported here are 2 orders of magnitude longer than typical MD simulations, and, thus, the possibility remains that an fcc structure is a short-lived metastable phase. In contrast with experiments performed on single crystals and MD simulations of the shock-induced transition in single crystals, we find that the observed c/a ratio in the polycrystalline case (1.61 ± 0.01) is close to the ideal hcp value and is in close agreement with values reported in DAC-based experiments. We interpret this as being due to the single crystals having few defects as sources to generate enough dislocations to relax on the time scale of the measurements, whereas, the grain boundaries and other defects in the rolled foil would act as sources for dislocations to relax the shear stress. However, it is clear that the detailed physics of plastic behavior under shock compression and ultrahigh-strain rate laser compression remains an area that needs to be investigated further, and time-resolved diffraction can play an important role in advancing our understanding of the underlying physical processes and time scales.

ACKNOWLEDGMENTS

The authors thank the staff at the Vulcan Laser Facility at the Rutherford Appleton Laboratory and are grateful for fruitful discussions with R. Smith, J. Eggert, and G. Collins. This work was performed under the auspices of the US Department of Energy by the Lawrence Livermore National Laboratory (LLNL) under Contract No. DE-AC52-07NA27344 supported by the LDRD program Project No. 06-SI-004 at LLNL. Additional support was provided by the UK EPSRC under Grant No. GR/R25699/01.

*hawreliak1@llnl.gov

[1] D. Bancroft, E. L. Peterson, and S. Minshall, J. Appl. Phys. **27**, 291 (1956).
[2] S. Minshall, Phys. Rev. **98**, 271 (1955).
[3] J. Walsh, Bull. Am. Phys. Soc. **29**, 28 (1954).
[4] J. Jamieson and A. W. Lawson, J. Appl. Phys. **33**, 776 (1962).
[5] H. Mao, W. A. Bassett, and T. Takahashi, J. Appl. Phys. **38**, 272 (1967).
[6] D. H. Kalantar, J. F. Belak, G. W. Collins, J. D. Colvin, H. M. Davies, J. H. Eggert, T. C. Germann, J. Hawreliak, B. L. Holian, K. Kadau *et al.*, Phys. Rev. Lett. **95**, 075502 (2005).
[7] J. Hawreliak, J. D. Colvin, J. H. Eggert, D. H. Kalantar, H. E. Lorenzana, J. S. Stolken, H. M. Davies, T. C. Germann, B. L. Holian, K. Kadau *et al.*, Phys. Rev. B **74**, 184107 (2006).
[8] F. M. Wang and R. Ingalls, Phys. Rev. B **57**, 5647 (1998).

[9]K. Kadau, T. C. Germann, P. S. Lomdahl, and B. L. Holian, Science **296**, 1681 (2002).
[10]K. Kadau, T. C. Germann, P. S. Lomdahl, and B. L. Holian, Phys. Rev. B **72**, 064120 (2005).
[11]K. Kadau, T. C. Germann, P. S. Lomdahl, R. C. Albers, J. S. Wark, A. Higginbotham, and B. L. Holian, Phys. Rev. Lett. **98**, 135701 (2007).
[12]K. Kadau, T. C. Germann, P. S. Lomdahl, R. C. Albers, J. S. Wark, A. Higginbotham, and B. L. Holian, AIP Conf. Proc. **955**, 313 (2007).
[13]C. N. Danson, L. J. Barzanti, Z. Chang, A. E. Damerell, C. B. Edwards, S. Hancock, M. H. R. Hutchinson, M. H. Key, S. Luan, and R. R. Mahadeo, Opt. Commun. **103**, 392 (1993).
[14]J. Hawreliak, H. E. Lorenzana, B. A. Remington, S. Lukezic, and J. S. Wark, Rev. Sci. Instrum. **78**, 083908 (2007).
[15]P. M. Celliers, G. W. Collins, L. B. Da Silva, D. M. Gold, and R. Cauble, Appl. Phys. Lett. **73**, 1320 (1998).
[16]J. C. Boettger and D. C. Wallace, Phys. Rev. B **55**, 2840 (1997).
[17]A. K. Singh, C. Balasingh, H.-k. Mao, R. J. Hemley, and J. Shu, J. Appl. Phys. **83**, 7567 (1998).
[18]A. K. Singh, H. P. Liermann, S. K. Saxena, H. K. Mao, and S. U. Devi, J. Phys. Condens. Matter **18**, 969 (2006).
[19]M. W. Guinan and D. N. Beshers, J. Phys. Chem. Solids **29**, 541 (1968).
[20]P. Söderlind, J. A. Moriarty, and J. M. Wills, Phys. Rev. B **53**, 14063 (1996).
[21]J. M. Brown, J. N. Fritz, and R. S. Hixson, J. Appl. Phys. **88**, 5496 (2000).
[22]D. R. Bland, IMA J. Appl. Math. **1**, 56 (1965).
[23]J. Swegle and D. Grady, J. Appl. Phys. **58**, 692 (1985).
[24]G. Swan, G. Duvall, and C. Thornhill, J. Mech. Phys. Solids **21**, 215 (1973).
[25]B. J. Jensen, G. T. Gray III, and R. S. Hixson, J. Appl. Phys. **105**, 103502 (2009).